



HAL
open science

Oxidative stress contributes differentially to the pathophysiology of Charcot-Marie-Tooth disease type 2K

Julien Cassereau, Arnaud Chevrollier, Philippe Codron, Cyril Goizet, Naïg Gueguen, Christophe Verny, Pascal Reynier, Dominique Bonneau, Guy Lenaers, Vincent Procaccio

► To cite this version:

Julien Cassereau, Arnaud Chevrollier, Philippe Codron, Cyril Goizet, Naïg Gueguen, et al.. Oxidative stress contributes differentially to the pathophysiology of Charcot-Marie-Tooth disease type 2K. *Experimental Neurology*, 2020, 323, pp.113069. 10.1016/j.expneurol.2019.113069 . hal-02388209

HAL Id: hal-02388209

<https://univ-angers.hal.science/hal-02388209>

Submitted on 21 Dec 2021

HAL is a multi-disciplinary open access archive for the deposit and dissemination of scientific research documents, whether they are published or not. The documents may come from teaching and research institutions in France or abroad, or from public or private research centers.

L'archive ouverte pluridisciplinaire **HAL**, est destinée au dépôt et à la diffusion de documents scientifiques de niveau recherche, publiés ou non, émanant des établissements d'enseignement et de recherche français ou étrangers, des laboratoires publics ou privés.



Distributed under a Creative Commons Attribution - NonCommercial 4.0 International License

Oxidative stress contributes differentially to the pathophysiology of Charcot-Marie-Tooth disease type 2K

Julien Cassereau ^{a,b*§}, Arnaud Chevrollier ^{a§}, Philippe Codron ^{a,b}, Cyril Goizet ^c, Naïg Gueguen ^{a,d},
Christophe Verny ^{a,b}, Pascal Reynier ^{a,d}, Dominique Bonneau ^{a,d}, Guy Lenaers ^a, Vincent Procaccio ^{a,d}

a. MitoLab, UMR CNRS 6015-INSERM 1083, MitoVasc Institute, University of Angers, Angers, France

b. University Hospital of Angers, Department of Neurology, F-49100 Angers, France

c. Centre de Référence Neurogénétique, Service de Génétique, Hôpital Pellegrin, University Hospital of Bordeaux and Laboratoire MRGM, INSERM U1211, University of Bordeaux, F-33000 Bordeaux, France

d. University Hospital of Angers, Department of Biochemistry and Genetics, F-49100 Angers, France

*** Corresponding Author:**

Dr Julien Cassereau

MitoVasc Unit, INSERM U1083 CNRS 6015, Angers University, F-49100 Angers, France

University Hospital of Angers, Department of Neurology

4 rue Larrey, F-49100 Angers, France

Email : jucassereau@chu-angers.fr (JC)

§ These authors equally contributed to this work

Running Title: Oxidative stress in Charcot-Marie-Tooth disease type 2K

Declarations of interest: none.

Title: 94 characters

Abstract: 177 words

Manuscript: 3683 words.

References: 40, **Figures:** 5, **Table:** 1, supplementary figures or tables: 4

Abstract

Charcot-Marie-Tooth (CMT) disease is a common inherited peripheral neuropathy. The CMT2K axonal form is associated with *GDAP1* dominant mutations, which according to the affected domain cause a gradient of severity. Indeed, the p.C240Y mutation, located within *GDAP1* glutathione S-transferase (GST) domain and associated to a mitochondrial complex I defect, is related to a faster disease progression, compared to other mutations, such as the p.R120W located outside the GST domain. Here, we analysed the pathophysiology of six CMT2K fibroblast cell lines, carrying either the p.C240Y or p.R120W mutations. We show that complex I deficiency leads to a redox potential alteration and a significant reduction of sirtuin 1 (SIRT1) expression, a major deacetylase sensitive to the cellular redox state, and NRF1 the downstream target of SIRT1. In addition, we disclosed that the p.C240Y mutation is associated with a greater mitochondrial oxidative stress than the p.R120W mutation. Moreover, complex I activity is further restored in CMT2K mutant cell lines exposed to resveratrol. Together, these results suggest that the reduction of oxidative stress may constitute a promising therapeutic strategy for CMT2K.

Keywords: Charcot-Marie-Tooth, *GDAP1*, mitochondria, complex I, oxidative stress.

1. Introduction

Charcot-Marie-Tooth (CMT) disease is a common inherited peripheral neuropathy with a prevalence of about 10-30 per 100,000 population, depending on the country of origin (Emery, 1991). To date, more than 80 genes are associated with CMT (Timmerman, et al., 2014), many of them encoding mitochondrial proteins, among which the mitofusin 2 (MFN2) and ganglioside-induced differentiation-associated-protein 1 (GDAP1). GDAP1 mutations are responsible for CMT4A [MIM:214400], the most frequent recessive subtype of demyelinating CMT; for ARCMT2 [MIM:607706], the axonal recessive subtype; for CMTRIA [MIM:608340], the intermediate recessive CMT; and for CMT2K [MIM:607831], the rare dominant subtype. These different forms encompass a large phenotypic variability (Cassereau, et al., 2011).

Although GDAP1 protein is known to be involved in mitochondrial morphology and function (Rzepnikowska and Kochanski, 2018), the pathophysiology of CMT2K is not fully understood. Structurally, GDAP1 belongs to the glutathione S-transferase (GST) family (Cuesta, et al., 2002, Marco, et al., 2004) and it was recently shown that recombinant GDAP1 has a theta-class-like GST activity regulated by its C-terminal hydrophobic domain 1 (HD1), in an autoinhibitory manner (Huber, et al., 2016). GDAP1, which is upregulated by oxidative stress, also regulates cellular glutathione (GSH) content *in vivo*, and protects cells against oxidative stress in HT22 mouse neuronal cells, whereas GDAP1 knockdown increases the susceptibility of the NSC34 motor neuron-like cells against GSH depletion (Noack, et al., 2012). In this respect, CMT4A fibroblasts have reduced GDAP1 levels, reduced GSH concentrations and a reduced mitochondrial membrane potential, suggesting that oxidative stress acts as a key player in the pathogenesis of this specific CMT (Noack, et al., 2012). This is reinforced by the fact that *GDAP1* knockout mice (*Gdap1*^{-/-}) present a mild and persistent

oxidative stress in the peripheral nervous system, which is compensated in the central nervous system by the expression of the GDAP1 paralogue named GDAP1L1 (Niemann, et al., 2014). In addition, patient skin fibroblasts carrying the heterozygous GDAP1:p.C240Y mutation show a defective mitochondrial complex I (CI) activity, highlighting the role of GDAP1 in mitochondrial bioenergetics (Cassereau, et al., 2009). CI deficiency, the commonest enzymatic defect of the oxidative phosphorylation (OXPHOS) system (Smeitink and van den Heuvel, 1999, Triepels, et al., 2001), is associated with a large spectrum of disorders ranging from Leigh's disease, Leber's hereditary optic neuropathy, mitochondrial encephalomyopathy with lactic acidosis and stroke-like episodes (MELAS) to other devastating neurodegenerative disorders, including Parkinson's disease (Schapira, et al., 1990). CI deficiency leads to reduced NADH oxidation, decreased electron transfer and Reactive Oxygen Species (ROS) overproduction, altogether cutting down mitochondrial ATP production (Kussmaul and Hirst, 2006), and increasing cellular damage (Fridovich, 1997).

The present study, carried out on skin fibroblasts from a series of CMT2K patients of two unrelated *GDAP1* families harboring either the p.C240Y or the p.R120W mutation, investigates the metabolic and the oxidative stress consequences of these respective mutations affecting or not the GDAP1 GST domain.

2. Material and Methods

2.1. Cell cultures

Primary skin fibroblasts were obtained from biopsies performed after written consent from six CMT2K patients, three with the GDAP1:p.C240Y mutation, three with the GDAP1:p.R120W mutation, and three control subjects (Supplementary Fig.1). Fibroblasts were maintained in 10% DMEM bovine calf serum (BCS) at 37°C in a humidified atmosphere with 5% CO₂. All fibroblast cultures were mycoplasma-free, as shown by the DAPI/Hoechst *in situ* coloration

and by PCR (Venor®Gem, BioValley, Marne-la-Vallée, France). All experiments were carried out on cells with similar passage numbers, ranging from 5 to 15, to avoid artefacts due to senescence.

For experiments using resveratrol, control vehicle (ethanol 1:2500) and 10µM or 25µM resveratrol (Sigma Chemicals St Louis, MO, USA) were added 48 hours before performing measurements.

2.2. Mitochondrial DNA sequencing

To exclude the contribution of mitochondrial DNA (mtDNA) mutations, we sequenced the entire mitochondrial genome of each cell line as described elsewhere (Nochez, et al., 2009).

2.3. Measurement of the respiratory rates and efficiency of mitochondrial ATP production in permeabilized cells

The respiratory rates were determined in cells permeabilized, by treatment with digitonin (15 µg/million cells). Cells were resuspended in the respiratory buffer (10 mM KH₂PO₄, 300 mM mannitol, 10 mM KCl and 5 mM MgCl₂, pH 7.4). The respiratory rates of 3-5*10⁶ cells were recorded at 37°C in 1.5 ml glass chambers using a two-channel, high-resolution Oxygraph respirometer (Oroboros, Innsbruck, Austria) as described elsewhere (Desquirit-Dumas, et al., 2012). Briefly, respiration was initiated with complex I substrates (5 mM malate and 5 mM pyruvate). Complex I-coupled state 3 respiration was measured by adding 0.5 mM NAD⁺ or 1.5 mM ADP. Next, 10 mM succinate was added to reach maximal coupled respiration, and 10 µM rotenone were injected to obtain the complex II-coupled state 3 respiration. Oligomycin (8 µg/ml) was added to determine the uncoupled state 4 respiration. Finally, FCCP (1 µM) was added to control the permeabilisation of fibroblasts.

The rate of mitochondrial ATP synthesis and the ATP/O ratio were determined in digitonin permeabilized cells as described elsewhere (Loiseau, et al., 2007).

2.4. Enzymatic activities

The activity of the mitochondrial OXPHOS complex was measured on cell homogenates using a Beckman DU 640 spectrophotometer (Beckman Coulter, Fullerton, CA, USA) with a minor adaptation of the method described by Rustin et al. (Rustin, et al., 1994). Complex I (NADH ubiquinone reductase) activity was measured according to the procedure described elsewhere (Loiseau, et al., 2007), modified by Benit et al. (Benit, et al., 2008) with the use of 2,6-dichlorophenolindophenol (DCPIP). Aconitase and fumarase activities were determined as described elsewhere (Razmara, et al., 2008). Isocitrate dehydrogenase activity was measured by following the appearance of NADH using 0.8 mM NAD⁺ and NADP⁺ and 10 mM isocitrate as substrates in a mixture containing 2 mM CaCl₂, 0.2 mM EDTA and 10 mM MgCl₂, in 50 mM KH₂PO₄ buffer, pH 7.5.

2.5. Lactate and pyruvate concentrations in the cell supernatant

Lactate concentrations in the culture media were determined by spectrophotometry, using enzymatic assays (Boehringer, Mannheim, Germany) on a Hitachi-Roche apparatus (Roche Diagnostics GmbH, Mannheim, Germany). Pyruvate concentration was determined by measuring the decrease in the NADH concentration in the presence of the lactate dehydrogenase enzyme using the DiaSys enzymatic kit (DiaSys, Holzheim, Germany).

2.6. Determination of membrane protein thiol content

The mitochondrial suspension, incubated in a standard reaction medium, was submitted to two subsequent freeze-thawing procedures to release matrix proteins before centrifugation for 2 min at 16,000 rpm. The pellet was treated with 200 µl of 6% trichloroacetic acid and

centrifuged at 16,000 rpm for 2 min in order to precipitate the proteins. The final pellet was resuspended in 200 µl of a medium containing 5 mM EDTA, antiprotease, 0.1% triton, and neutralized with 1-2 µl of 5M KOH. 50 µl of protein were added to 950 µl of a solution containing 5,5'-dithio-bis (2-nitrobenzoic acid) (DTNB) 1mM, KH₂PO₄ 0.1 M (pH 7.2) and 1 mM EDTA. The solution was incubated for 15 min at 37°C before measurement. The absorption was measured at 412 nm.

2.7. Western-blotting and blue native polyacrylamide gel electrophoresis of complex I

Isolated mitochondria were extracted from fibroblasts according to the protocol as described previously (Leman, et al., 2015). Mitochondrial proteins (20 µg) were denatured in Laemmli buffer and analysed by Western blotting using an anti-voltage-dependent anion channel (VDAC, 1:1000, Abcam), anti-NDUFB8 (1:500, Abcam, Cambridge, UK), anti-SIRT1 and anti-SIRT3 (1:1000, Cell Signaling Technology, Beverly; MA, USA), anti-MnSOD (1:1000, Abcam), anti-NRF1 (1:500, Santa Cruz Biotechnology, Germany), anti-alpha-tubulin (1:10,000, Sigma, St Louis, MO, USA). Membranes were washed three times in 0.1% TBS-Tween and incubated with anti-mouse IgG horseradish peroxidase-linked antibody (1:20,000, Amersham Biosciences, Buckinghamshire, UK) or with goat anti-rabbit HRP conjugate (1:20,000, Bio-Rad, Hercules, CA, USA) for 1h at room temperature. The immunoreactive proteins were visualized with enhanced chemiluminescence (ECL+ Western Blotting Detection Reagents, Amersham Biosciences, Buckinghamshire, UK). Band intensities were quantified with Quantity One software (Bio-Rad, Hercules, CA, USA).

Blue native polyacrylamide gel electrophoresis (BN-PAGE) was performed as described elsewhere (Wittig, et al., 2006) using antibodies against NDUFB6, NDUFS3 and NDUFA9 subunits (Abcam).

2.8. Deconvolution microscopy: mitochondrial network analysis, mitochondrial membrane potential and ROS detection

Mitochondria were labelled using Mitotracker® Green (Molecular Probes, CA, USA). Fibroblasts were pulse-loaded with 100nM Mitotracker® Green for 15 min in a humidified atmosphere (95% air, 5% CO₂) at 37°C. Images were acquired with an inverted wide-field Leica (DMI6000B, Microsystems, Wetzlar, Germany) equipped with a Roper CoolSnap HQ2 camera (Roper Scientific, Tucson, AZ, USA), a high-sensitivity CCD camera for quantitative fluorescence microscopy. 3D processing and morphometric analysis were done with Imaris 8.1® software (Bitplane, Zurich, Switzerland).

To evaluate ROS production, cells were cultured in a four-well chamber slide (Labtek, Nunc International, Naperville, IL, USA). After 48 hours of culture, cells were washed with Hank's buffered salt solution (HBSS), incubated with 5µM MitoSOX™ (Molecular Probes) for 15 min at 37°C. For each patient, 30 cells were analysed by creating 80 equal regions (Metamorph® 7.10 software, Molecular Devices, San Jose, CA, USA), 70 of which were positioned over mitochondria, the remaining 10 over the cytosol to evaluate the background noise. Subtraction of the background noise from the average intensity of fluorescence allowed the qualitative and quantitative comparison of the production of mitochondrial ROS in cells from CMT2K patients and controls.

Mitochondrial membrane potential measurement- Cells were stained with 50nM TMRM (Thermo Fisher Scientific, Waltham, MA, USA) to measure mitochondrial delta psi and 100 nM Mitotraker green to control mitochondrial content and subjected to the inverted wide-field microscope for visualization (Metamorph). To normalize the variations due to differences between mitochondrial densities, the ratio of TMRM/ Mitotraker intensities was calculated in individual cells. Data are presented as mean of three independent experiments.

2.9. Statistical analysis

Statistical analyses were carried out using PRISM software version 5.0 for Windows (GraphPad, La Jolla, CA). Comparisons of two unpaired groups were performed using non parametric Mann-Whitney U test. Differences were considered to be significant at $p < 0.05$.

2.10. Ethical considerations

The study protocol has been approved by the Regional Ethics Committee West II (Authorization Number AC-2012-1507). An anonymous database and a list of correspondence have been generated and stored in the datacenter of the University Hospital of Angers with restricted access.

3. Results

3.1. Fibroblasts from *CMT2K* patients have a mitochondrial complex I (CI) deficiency

CI enzymatic activity was about 50% lower in the p.C240Y fibroblasts compared to controls (Fig. 1a, $p=0.01$), while only reduced by 30% in the p.R120W fibroblasts (Fig. 1a, $p=0.09$). Measurements of mitochondrial oxygen consumption revealed that using CI malate-pyruvate (MP) substrates, the respiratory rate (Fig. 1b) and the corresponding ATP production (Fig. 1c) were significantly lower in both mutant cell lines, compared to controls (40%, $p < 0.05$ in both measurements). Nevertheless, all the other respiratory complex enzymatic activities were normal in *CMT2K* fibroblasts (Supplementary Table 1), highlighting a specificity in the alteration of the CI function.

The metabolite indicator method, i.e., the lactate/pyruvate ratio, is commonly used to estimate the cytosolic NAD(H)-redox state (Sun, et al., 2012). The lactate/pyruvate ratio (L/P) in culture media, was altered in the p.C240Y and p.R120W fibroblasts, with a L/P ratio three

times higher in patient fibroblasts carrying the p.C240Y mutation ($p=0.025$) but not significant for the p.R120W mutation, compared to controls ($p=0.088$). These results highlight a significant change in the cytosolic NADH/NAD⁺ ratio in fibroblasts harboring a mutation in the GST domain compared to patient fibroblasts with a mutation outside of this domain (Fig. 1d). This NADH/NAD⁺ imbalance could be due to the significant reduction of CI activity in mutant cells.

3.2. The expression level of Sirt1 is reduced in CMT2K fibroblasts

As CI is regulated by acetylation involving sirtuins (SIRT), a conserved family of NAD-dependent deacetylases, we assessed the expression of SIRT1 and SIRT3, the first regulating mitochondrial biogenesis and metabolism, the latter being the main NAD⁺-dependent deacetylase into mitochondria. Western-blotting analysis revealed that SIRT1 levels were almost 70% lower in CMT2K mutant fibroblasts compared to controls (Fig. 2a, $p<0.05$), whereas the SIRT3 levels remained unchanged (Fig. 2b).

We performed western blotting to assess the expression of NRF1, a downstream effector of SIRT1 in 3 patients harboring the p.C240Y mutation and 1 patient harboring the p.R120W mutation. The expression of NRF1 was decreased both in patient fibroblasts harboring the p.C240Y and p.R120W mutations (Fig.2c, $p< 0.05$), in the same proportion of SIRT1 expression.

3.3. Complex I deficiency is not due to a defect in complex assembly.

Despite a reduction of SIRT1 protein expression, we did not observe a reduction of the CI subunits expression in CMT2K fibroblasts compared to controls. Indeed, NDUF8 CI subunit expression was unchanged in CMT2K fibroblasts related to control could reflect reduced CI

enzymatic activity (Fig. 3a). In addition, the analysis by Blue Native PAGE of CMT2K fibroblasts compared to controls did not reveal any defect in CI assembly (Fig. 3b).

3.4. The Krebs cycle is not responsible for CI defect

Despite a mitochondrial energetic defect, citrate synthase and other enzymes of the Krebs cycle, such as Isocitrate Dehydrogenase (IDH) and fumarase, did not show any significant variation in their activity (Table 1). Interestingly, in the p.C240Y fibroblasts, aconitase activity was significantly reduced by 40%. Aconitase is specifically sensitive to the presence of mitochondrial ROS and the reduction of the aconitase/fumarase ratio is considered as a good marker of oxidative stress (Niemann, et al., 2009). Thus, in p.C240Y fibroblasts, the reduced aconitase/fumarase ratio is suggestive of ROS overproduction.

3.5. The pC240Y mutation affecting GDAP1 GST domain leads to ROS overproduction

Using a fluorescent probe specific for superoxide anions (MitoSOXTM), we identified a 40% enhancement of fluorescence intensity in p.C240Y fibroblasts compared to controls (Fig. 4a and 4b, $p=0.020$). In addition, we observed a 50% decrease in thiol group level, which are the ROS targets, further supporting ROS overproduction (Fig. 4c, $p=0.015$). Moreover, the expression of manganese superoxide dismutase (MnSOD), a major mitochondrial antioxidant, was 53% higher in p.C240Y fibroblasts compared to controls (Fig. 4d, $p=0.045$). In contrast, in the p.R120W fibroblasts, no evidence of oxidative stress was observed (Fig. 4).

Mitochondrial membrane potential measured by TMRM in p.C240Y fibroblasts was normal compared to controls (Supplementary Fig.2). Moreover, no alteration of the mitochondrial network was shown in fibroblasts from patients harboring the p.R120W mutation

(Supplementary Fig.3) in contrast with patients carrying the p.C240Y mutation, as previously shown (Cassereau et al., 2009).

These results show that the p.C240Y mutation in GDAP1 GST domain significantly increases mitochondrial oxidative stress, thus highlighting a defect in GST activity. These results strongly suggest that ROS overproduction depends on the mutation location and might modulate CMT2K pathophysiology.

3.6. Resveratrol restores complex I activity in CMT2K fibroblasts

Since oxidative stress is a significant modulator of CMT2K pathophysiology, we evaluated the effect of resveratrol, an antioxidant acting on CI activity and promoting mitochondrial superoxide dismutase activity and biogenesis.

CMT2K fibroblasts carrying the p.C240Y and p.R120W mutations were treated with 10 μ M or 25 μ M resveratrol. Resveratrol 50 μ M was not used in CI activity analysis since an antiproliferative effect was observed at this concentration in control and CMT2K fibroblasts (data not shown). Whereas treatment with 10 μ M resveratrol produced no significant modification of CI activity (data not shown), treatment with 25 μ M resveratrol modulated CI activity in CMT2K fibroblasts with a trend towards the restoration of CI activity in both p.C240Y and p.R120W fibroblasts. We also assessed the effect of resveratrol in alleviating mitochondrial dysfunction in cells carrying GDAP1 mutations independently of the location and mutation type in the perspective of potential future therapeutic studies on CMT2K patients. Combining both patient families showed a significant improvement of CI activity after resveratrol treatment (Fig. 5, $p < 0.05$).

4. Discussion

An analysis of the literature (Cassereau, et al., 2011, Cassereau, et al., 2009, Chung, et al., 2008, Claramunt, et al., 2005, Crimella, et al., 2010, Sivera, et al., 2010) shows that in CMT2K patients the position of the mutation affecting GDAP1 primary structure is associated with the severity of the clinical presentation. Indeed, missense mutations located inside the GST domain induce a faster progression of the disease, compared to mutations located outside the GST domain, emphasizing the key role of these domains in GDAP1 function.

In this study, we performed a detailed functional assessment of the mitochondrial respiratory chain in fibroblasts from six CMT2K patients from two unrelated families. Three patients from the first family harbored the p.C240Y mutation, and 3 patients from the second family carried the p.R120W mutation.

Globally, we found that CMT2K fibroblasts presented an alteration of the cytosolic NADH/NAD⁺ ratio, suggesting a mitochondrial dysfunction. We confirmed a selective defect in CI-mediated respiration in all *GDAP1* cells and a defect of CI enzymatic activity in cells from the family harboring the p.C240Y mutation, whereas the decreased CI enzymatic activity was not significant in the second family, suggesting a secondary CI defect. In addition, no defective CI assembly was evidenced in CMT2K fibroblasts, nor was reduced the CI level. The presence of structural domains related to the cytosolic GSTs in GDAP1 suggests that GDAP1 plays a protective role against oxidative stress. Recently, a GST activity was demonstrated for GDAP1, regulated by its C-terminal HD1 domain in an autoinhibitory manner (Huber, et al., 2016). It was further shown that GDAP1 regulates cellular glutathione content (Noack, et al., 2012). GSTs are widely distributed, present both in plants and animals, and play a role in the detoxification of xenobiotics and endogenous toxicants. The primary catalytic activity of GSTs is the conjugation of electrophilic compounds through nucleophilic attack by reduced glutathione (GSH). The defect of this process would lead to increased ROS

damages, as free radicals have been associated with deleterious effects on lipid peroxidation, and on protein oxidation of CI (Ketterer, et al., 1988, Zhao, et al., 1999). This sets up a vicious circle in which CI is not only the source, but also the target of free radicals. Moreover, dominant *GDAP1* mutations induce ROS production and trigger apoptosis (Niemann, et al., 2009), supporting the hypothesis that overproduction of ROS contributes to CMT2K pathogenesis.

Interestingly, in our study, we identified a significant oxidative stress only in fibroblasts carrying the p.C240Y mutation as seen with the reduced aconitase/fumarase ratio, whereas those carrying the p.R120W mutation had the same level of oxidative stress as control cells. Aconitase is a mitochondrial enzyme with an iron-sulfur center that is acutely sensitive to inactivation by superoxide. The aconitase/fumarase ratio was used in our study as an indicator of mitochondrial ROS exposure since ROS decrease aconitase activity, but without interfering with fumarase activity, the latter lacking iron/sulfur clusters (Niemann, et al., 2009).

These results suggest that ROS involvement in the pathophysiology of CMT2K depends on the mutation location, and rules out the hypothesis of a defect in electron transport to explain the CI deficiency. Therefore, we raise the hypothesis that *GDAP1* plays a potential role against oxidative stress, which may be affected by mutations located into the GST domains. This is reinforced by the fact that three quarters of *GDAP1* mutations affect the GST domains, suggesting an important role of these domains in preventing the evolution of the disease (Cassereau, et al., 2011, Crimella, et al., 2010).

Because CI accepts electrons from NADH produced by the Krebs cycle, we monitored the activities of the isocitrate dehydrogenase and citrate synthase, without finding evidence for any alteration, suggesting that the Krebs cycle was not involved in CI defects that we observed.

It has been shown in both healthy and pathological conditions that ROS-induced signalling pathways are involved in controlling CI function by sirtuin mediated acetylation (Koopman, et al., 2010). Sirtuins are a conserved family of NAD-dependent deacetylases that regulate the cell metabolism by the deacetylation of key enzymes, among which some governing the mitochondrial biogenesis and activity, and others involved in the regulation of survival, stress and metabolism pathways (Sauve, et al., 2006). Sirtuins are also emerging as potential actors involved in various neurodegenerative conditions such as Alzheimer and Parkinson's disease, thus suggesting that modulation of their activity could provide some routes to therapies. Using *Sirt3*-deficient mice, it was shown that SIRT3 is the major mitochondrial deacetylase controlling the acetylation levels of mitochondrial proteins among which CI subunits (Ahn, et al., 2008). Sirt3 can also physically interact with CI subunits such as NDUFA9, and regulate their enzymatic activity, thus positioning mitochondrial protein acetylation as an important regulatory pathway of CI activity.

SIRT1, a cytoplasmic redox sensitive deacetylase, has a primary role in mitochondrial metabolism promoting mitochondrial biogenesis, by activating the PPARgamma coactivator-1alpha (PGC1 α) and the nuclear respiratory factor 1 (NRF1) regulatory pathways (Pfluger, et al., 2008). SIRT1 enzymatic activity is regulated by multiple factors including the NAD⁺/NADH ratio (Fulco, et al., 2003). Western-blotting analyses, revealed a significant reduction of the expression of both SIRT1 and NRF1 in CMT2K mutant fibroblasts whereas SIRT3 levels were unaffected. These results emphasize that SIRT1 could be regulated by GDAP1 activity contributing to the bioenergetic dysfunction of CMT2K mutant cells. Interestingly, SIRT1 is activated by resveratrol, a polyphenol phytoalexin, present in red wine and grapes (Borra, et al., 2005). Furthermore, resveratrol has an antioxidant activity increasing superoxide dismutase mitochondrial activity and protein expression in mitochondria (Robb, et

al., 2008). In this respect, resveratrol improves mitochondrial complex activities during cerebral ischemia (Yousuf, et al., 2009).

Since oxidative stress is involved in the pathophysiology of CMT2K, depending on the mutation location, we evaluated the effect of an antioxidant treatment on CI activity. Because SIRT1 expression was drastically reduced in CMT2K fibroblasts, we selected resveratrol for its antioxidant and SIRT1-activator properties, and for its role in mitochondrial metabolism. Interestingly, CI activity was increased in all tested CMT2K fibroblasts, suggesting that resveratrol activates SIRT1 and restores CI activity in CMT2K mutant cells. Further studies are needed to identify the mechanisms involved in regulating CI activity.

5. Conclusions

In conclusion, this study provides further evidence for the critical role of mitochondrial dysfunction in the pathogenesis of CMT2K associated with GDAP1 mutations. We confirmed that GDAP1 mutations lead to defective mitochondrial CI activity and disclosed that oxidative stress is part of the CMT2K pathophysiology. In this respect, mutation in one of the GST domains may adversely affect the antioxidant properties of GDAP1 and lead to greater mitochondrial oxidative stress and more severe clinical presentations than mutations located outside the GST domains. The oxidative stress reduction may thus constitute a promising therapeutic strategy against the consequences of mitochondrial dysfunction in CMT2K.

Acknowledgments

We are grateful to Jennifer Alban, Celine Wetterwald, Aurelie Renaud and Aurore Inisan for technical assistance and Kanaya Malkani for critical reading of the manuscript.

Funding

This work was supported by grants from the University Hospital of Angers, the Université d'Angers, the Région Pays de la Loire, Angers Loire Métropole, the Fondation Maladies Rares, and the *Association contre les Maladies Mitochondriales* (AMMi).

References

1. Ahn, B. H., Kim, H. S., Song, S., Lee, I. H., Liu, J., Vassilopoulos, A., Deng, C. X., and Finkel, T., 2008. A role for the mitochondrial deacetylase Sirt3 in regulating energy homeostasis. *Proc Natl Acad Sci U S A* 105, 14447-14452.
2. Benit, P., Slama, A., and Rustin, P., 2008. Decylubiquinol impedes mitochondrial respiratory chain complex I activity. *Molecular and Cellular Biochemistry* 314, 45-50.
3. Borra, M. T., Smith, B. C., and Denu, J. M., 2005. Mechanism of human SIRT1 activation by resveratrol. *Journal of biological chemistry* 280, 17187-17195.
4. Cassereau, J., Chevrollier, A., Bonneau, D., Verny, C., Procaccio, V., Reynier, P., and Ferre, M., 2011. A locus-specific database for mutations in GDAP1 allows analysis of genotype-phenotype correlations in Charcot-Marie-Tooth diseases type 4A and 2K. *Orphanet journal of rare diseases* 6, 87.
5. Cassereau, J., Chevrollier, A., Gueguen, N., Desquiret, V., Verny, C., Nicolas, G., Dubas, F., Amati-Bonneau, P., Reynier, P., Bonneau, D., and Procaccio, V., 2011. Mitochondrial dysfunction and pathophysiology of Charcot-Marie-Tooth disease involving GDAP1 mutations. *Experimental neurology* 227, 31-41.
6. Cassereau, J., Chevrollier, A., Gueguen, N., Malinge, M. C., Letournel, F., Nicolas, G., Richard, L., Ferre, M., Verny, C., Dubas, F., Procaccio, V., Amati-Bonneau, P., Bonneau, D., and Reynier, P., 2009. Mitochondrial complex I deficiency in GDAP1-related autosomal dominant Charcot-Marie-Tooth disease (CMT2K). *Neurogenetics* 10, 145-150.
7. Chung, K. W., Kim, S. M., Sunwoo, I. N., Cho, S. Y., Hwang, S. J., Kim, J., Kang, S. H., Park, K. D., Choi, K. G., Choi, I. S., and Choi, B. O., 2008. A novel GDAP1 Q218E mutation in autosomal dominant Charcot-Marie-Tooth disease. *J Hum Genet* 53, 360-364.
8. Claramunt, R., Pedrola, L., Sevilla, T., Lopez de Munain, A., Berciano, J., Cuesta, A., Sanchez-Navarro, B., Millan, J. M., Saifi, G. M., Lupski, J. R., Vilchez, J. J., Espinos, C., and Palau, F., 2005. Genetics of Charcot-Marie-Tooth disease type 4A: mutations, inheritance, phenotypic variability, and founder effect. *J Med Genet* 42, 358-365.
9. Crimella, C., Tonelli, A., Airoidi, G., Baschiroto, C., D'Angelo, M. G., Bonato, S., Losito, L., Trabacca, A., Bresolin, N., and Bassi, M. T., 2010. The GST domain of GDAP1 is a frequent target of mutations in the dominant form of axonal Charcot Marie Tooth type 2K. *J Med Genet* 47, 712-716.
10. Cuesta, A., Pedrola, L., Sevilla, T., Garcia-Planells, J., Chumillas, M. J., Mayordomo, F., LeGuern, E., Marin, I., Vilchez, J. J., and Palau, F., 2002. The gene encoding ganglioside-induced differentiation-associated protein 1 is mutated in axonal Charcot-Marie-Tooth type 4A disease. *Nat Genet* 30, 22-25.
11. Desquiret-Dumas, V., Gueguen, N., Barth, M., Chevrollier, A., Hancock, S., Wallace, D. C., Amati-Bonneau, P., Henrion, D., Bonneau, D., Reynier, P., and Procaccio, V., 2012. Metabolically induced heteroplasmy shifting and l-arginine treatment reduce the energetic defect in a neuronal-like model of MELAS. *Biochimica et Biophysica Acta* 1822, 1019-1029.
12. Emery, A. E., 1991. Population frequencies of inherited neuromuscular diseases--a world survey. *Neuromuscul Disord* 1, 19-29.
13. Fridovich, I., 1997. Superoxide anion radical (O₂⁻), superoxide dismutases, and related matters. *J Biol Chem* 272, 18515-18517.
14. Fulco, M., Schiltz, R. L., Iezzi, S., King, M. T., Zhao, P., Kashiwaya, Y., Hoffman, E., Veech, R. L., and Sartorelli, V., 2003. Sir2 regulates skeletal muscle differentiation as a potential sensor of the redox state. *Molecular cell* 12, 51-62.

15. Huber, N., Bieniossek, C., Wagner, K. M., Elsasser, H. P., Suter, U., Berger, I., and Niemann, A., 2016. Glutathione-conjugating and membrane-remodeling activity of GDAP1 relies on amphipathic C-terminal domain. *Scientific reports* 6, 36930.
16. Ketterer, B., Meyer, D. J., and Tan, K. H., 1988. The role of glutathione transferase in the detoxication and repair of lipid and DNA hydroperoxides. *Basic Life Sci* 49, 669-674.
17. Koopman, W. J., Nijtmans, L. G., Dieteren, C. E., Roestenberg, P., Valsecchi, F., Smeitink, J. A., and Willems, P. H., 2010. Mammalian Mitochondrial Complex I: Biogenesis, Regulation and Reactive Oxygen Species Generation. *Antioxid Redox Signal*.
18. Kussmaul, L., and Hirst, J., 2006. The mechanism of superoxide production by NADH:ubiquinone oxidoreductase (complex I) from bovine heart mitochondria. *Proceedings of the National Academy of Sciences of the United States of America* 103, 7607-7612.
19. Leman, G., Gueguen, N., Desquiret-Dumas, V., Kane, M. S., Wetterval, C., Chupin, S., Chevrollier, A., Lebre, A. S., Bonnefont, J. P., Barth, M., Amati-Bonneau, P., Verny, C., Henrion, D., Bonneau, D., Reynier, P., and Procaccio, V., 2015. Assembly defects induce oxidative stress in inherited mitochondrial complex I deficiency. *The international journal of biochemistry & cell biology* 65, 91-103.
20. Loiseau, D., Chevrollier, A., Verny, C., Guillet, V., Gueguen, N., Pou de Crescenzo, M. A., Ferre, M., Malinge, M. C., Guichet, A., Nicolas, G., Amati-Bonneau, P., Malthiery, Y., Bonneau, D., and Reynier, P., 2007. Mitochondrial coupling defect in Charcot-Marie-Tooth type 2A disease. *Ann Neurol* 61, 315-323.
21. Marco, A., Cuesta, A., Pedrola, L., Palau, F., and Marin, I., 2004. Evolutionary and structural analyses of GDAP1, involved in Charcot-Marie-Tooth disease, characterize a novel class of glutathione transferase-related genes. *Mol Biol Evol* 21, 176-187.
22. Niemann, A., Huber, N., Wagner, K. M., Somandin, C., Horn, M., Lebrun-Julien, F., Angst, B., Pereira, J. A., Halfter, H., Welzl, H., Feltri, M. L., Wrabetz, L., Young, P., Wessig, C., Toyka, K. V., and Suter, U., 2014. The Gdap1 knockout mouse mechanistically links redox control to Charcot-Marie-Tooth disease. *Brain : a journal of neurology* 137, 668-682.
23. Niemann, A., Wagner, K. M., Ruegg, M., and Suter, U., 2009. GDAP1 mutations differ in their effects on mitochondrial dynamics and apoptosis depending on the mode of inheritance. *Neurobiol Dis* 36, 509-520.
24. Noack, R., Frede, S., Albrecht, P., Henke, N., Pfeiffer, A., Knoll, K., Dehmel, T., Meyer Zu Horste, G., Stettner, M., Kieseier, B. C., Summer, H., Golz, S., Kochanski, A., Wiedau-Pazos, M., Arnold, S., Lewerenz, J., and Methner, A., 2012. Charcot-Marie-Tooth disease CMT4A: GDAP1 increases cellular glutathione and the mitochondrial membrane potential. *Human Molecular Genetics* 21, 150-162.
25. Nochez, Y., Arsene, S., Gueguen, N., Chevrollier, A., Ferre, M., Guillet, V., Desquiret, V., Toutain, A., Bonneau, D., Procaccio, V., Amati-Bonneau, P., Pisella, P. J., and Reynier, P., 2009. Acute and late-onset optic atrophy due to a novel OPA1 mutation leading to a mitochondrial coupling defect. *Molecular vision* 15, 598-608.
26. Pfluger, P. T., Herranz, D., Velasco-Miguel, S., Serrano, M., and Tschop, M. H., 2008. Sirt1 protects against high-fat diet-induced metabolic damage. *Proc Natl Acad Sci U S A* 105, 9793-9798.
27. Razmara, A., Sunday, L., Stirone, C., Wang, X. B., Krause, D. N., Duckles, S. P., and Procaccio, V., 2008. Mitochondrial effects of estrogen are mediated by estrogen receptor alpha in brain endothelial cells. *The Journal of pharmacology and experimental therapeutics* 325, 782-790.

28. Robb, E. L., Winkelmolen, L., Visanji, N., Brotchie, J., and Stuart, J. A., 2008. Dietary resveratrol administration increases MnSOD expression and activity in mouse brain. *Biochem Biophys Res Commun* 372, 254-259.
29. Rustin, P., Chretien, D., Bourgeron, T., Gerard, B., Rotig, A., Saudubray, J. M., and Munnich, A., 1994. Biochemical and molecular investigations in respiratory chain deficiencies. *Clinica chimica acta; international journal of clinical chemistry* 228, 35-51.
30. Rzepnikowska, W., and Kochanski, A., 2018. A role for the GDAP1 gene in the molecular pathogenesis of CharcotMarieTooth disease. *Acta Neurobiologiae Experimentalis* 78, 1-13.
31. Sauve, A. A., Wolberger, C., Schramm, V. L., and Boeke, J. D., 2006. The biochemistry of sirtuins. *Annu Rev Biochem* 75, 435-465.
32. Schapira, A. H., Cooper, J. M., Dexter, D., Clark, J. B., Jenner, P., and Marsden, C. D., 1990. Mitochondrial complex I deficiency in Parkinson's disease. *J Neurochem* 54, 823-827.
33. Sivera, R., Espinos, C., Vilchez, J. J., Mas, F., Martinez-Rubio, D., Chumillas, M. J., Mayordomo, F., Muelas, N., Bataller, L., Palau, F., and Sevilla, T., 2010. Phenotypical features of the p.R120W mutation in the GDAP1 gene causing autosomal dominant Charcot-Marie-Tooth disease. *Journal of the peripheral nervous system : JPNS* 15, 334-344.
34. Smeitink, J., and van den Heuvel, L., 1999. Human mitochondrial complex I in health and disease. *Am J Hum Genet* 64, 1505-1510.
35. Sun, F., Dai, C., Xie, J., and Hu, X., 2012. Biochemical issues in estimation of cytosolic free NAD/NADH ratio. *PloS one* 7, e34525.
36. Timmerman, V., Strickland, A. V., and Zuchner, S., 2014. Genetics of Charcot-Marie-Tooth (CMT) Disease within the Frame of the Human Genome Project Success. *Genes* 5, 13-32.
37. Triepels, R. H., Van Den Heuvel, L. P., Trijbels, J. M., and Smeitink, J. A., 2001. Respiratory chain complex I deficiency. *Am J Med Genet* 106, 37-45.
38. Wittig, I., Braun, H. P., and Schagger, H., 2006. Blue native PAGE. *Nature protocols* 1, 418-428.
39. Yousuf, S., Atif, F., Ahmad, M., Hoda, N., Ishrat, T., Khan, B., and Islam, F., 2009. Resveratrol exerts its neuroprotective effect by modulating mitochondrial dysfunctions and associated cell death during cerebral ischemia. *Brain Res* 1250, 242-253.
40. Zhao, T., Singhal, S. S., Piper, J. T., Cheng, J., Pandya, U., Clark-Wronski, J., Awasthi, S., and Awasthi, Y. C., 1999. The role of human glutathione S-transferases hGSTA1-1 and hGSTA2-2 in protection against oxidative stress. *Arch Biochem Biophys* 367, 216-224.

Figure legends

Fig. 1: Biochemical measurements represented as boxplots. (a) CI enzymatic activity normalized with respect to citrate synthase (CS) activity. (b) Rate of oxygen consumption with CI substrates (malate and pyruvate). (c) Mitochondrial ATP production with CI substrates. Experiments were performed on control fibroblasts (n=4), fibroblasts from patients harboring the p.C240Y mutation (n=3) and the p.R120W mutation (n=3). Three independent replicates were performed for each sample. (d) Lactate/pyruvate (L/P) ratio analysed in the culture media of fibroblasts from patients carrying either the p.C240Y (n=3) or p.R120W (n=3) mutations and controls (n=6). Three independent replicates were performed. Statistical significance: * $p < 0.05$.

Fig. 2: Cellular redox status and sirtuin protein expression. (a) Expression of SIRT1 analysed by Western blotting in CMT2K fibroblasts harboring the p.C240Y mutation (n=2) and the p.R120W mutation (n=2) compared to control fibroblasts (n=4). (b) Expression of SIRT3 in CMT2K analysed by Western blotting in CMT2K fibroblasts harboring the p.C240Y mutation (n=3) and the p.R120W mutation (n=3) compared to control fibroblasts (n=4). (c) Expression of NRF1 analysed by Western blotting in CMT2K fibroblasts harboring the p.C240Y mutation (n=3) and the p.R120W mutation (n=1) compared to control fibroblasts (n=4). Four independent replicates were performed for each patient and α -tubulin was used as a marker of protein loading. Statistical significance: * $p < 0.05$ for each experiment.

Fig. 3: Analysis of complex I assembly. (a) Expression of CI analysed using antibodies against the NDUFB8 subunit and VDAC as mitochondrial marker. Representative blots for three controls and a series of six CMT2K patients are shown. (b) CI assembly analysis by BN-PAGE using antibodies against the NDUFS3, NDUFB6, NDUF9 subunits. Two independent experiments were performed for each patient.

Fig. 4: Quantification of ROS production. (a) Fluorescence microscopic imaging, using a fluorescent probe specific for mitochondrial oxygen species (MitoSOXTM). Representative images for controls compared to fibroblasts from CMT2K patients harboring the p.C240Y and p.R120W mutations. (b) Histogram representing fluorescence intensity in patient fibroblasts harboring the p.C240Y (n=3) or the p.R120W mutations (n=2) compared to control fibroblasts (n=3). Results are expressed as percentages of control values. (c) Membrane protein thiol content in patients harboring the p.C240Y mutation (n=3) or the p.R120W mutation (n=2) compared to control fibroblasts (n=5). (d) Expression of MnSOD in fibroblasts from p.C240Y patients (n=3), p.R120W patients (n=3) and control fibroblasts (n=3) analysed by 3 independent Western blotting using α -tubulin as a marker of protein loading. Statistical significance: * p <0.05 for each experiment.

Fig. 5: Effect of 25 μ M resveratrol on complex I activity. CI enzymatic activity was normalized with respect to citrate synthase (CS) activity. Vehicle (V) corresponds to ethanol (dilution of 1:2500). R25 corresponds to treatment with 25 μ M resveratrol.

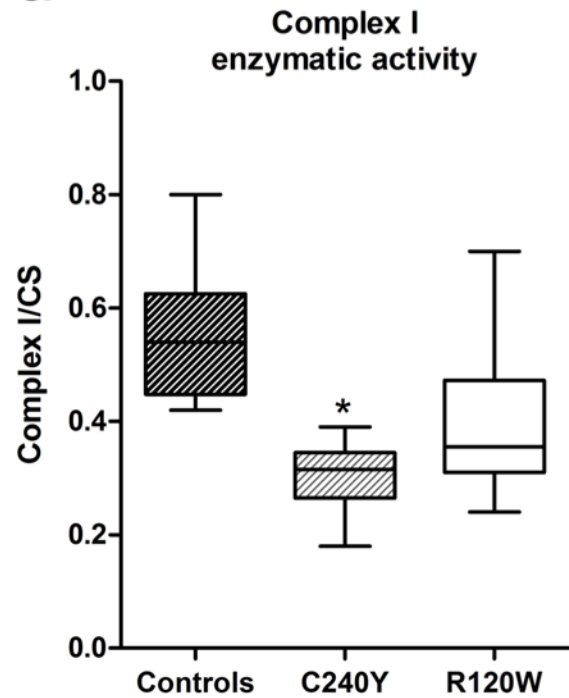
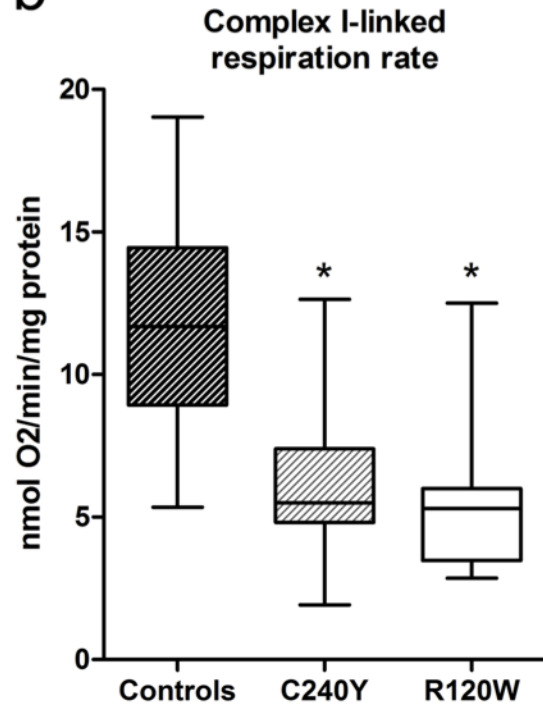
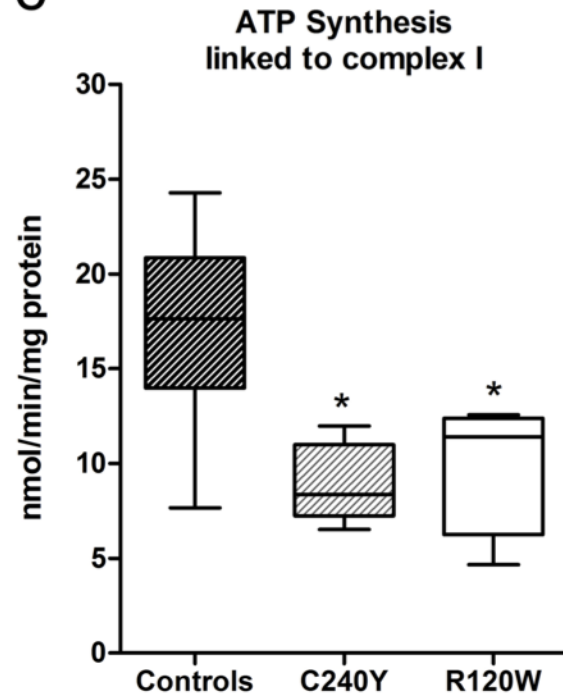
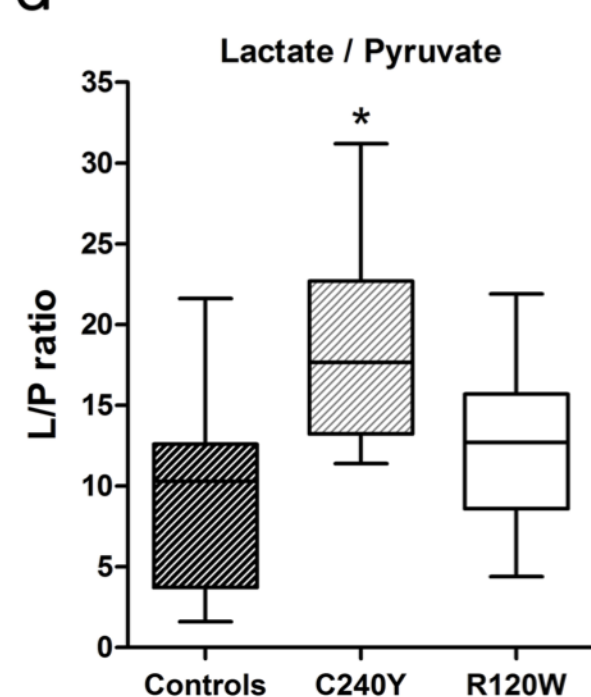
Three independent measurements were made on fibroblasts harboring the p.C240Y mutation (n=2), the p.R120W mutation (n=2), and controls (n=4). Results are expressed as mean values \pm standard deviation of three independent measurements. Statistical significance level: * p <0.05

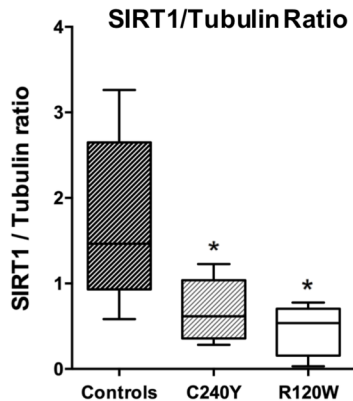
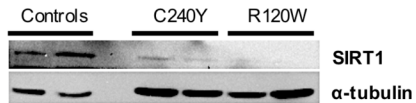
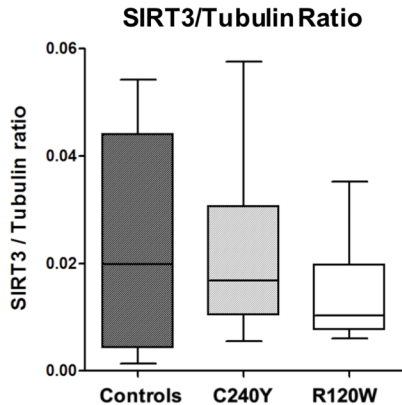
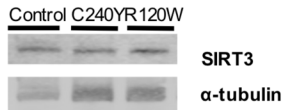
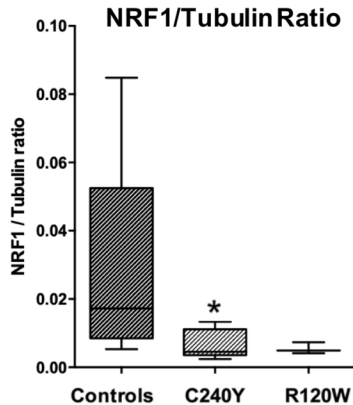
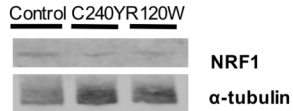
Table

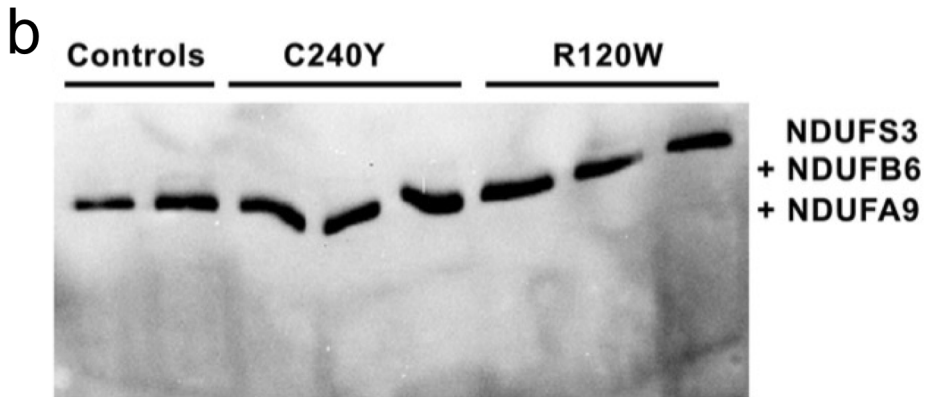
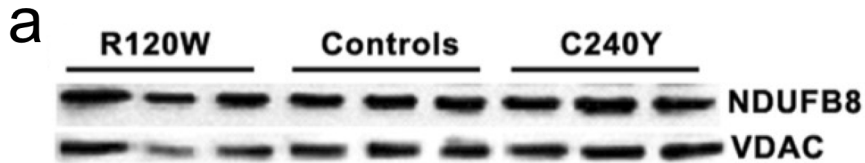
Table 1: Assessment of the Krebs cycle integrity.

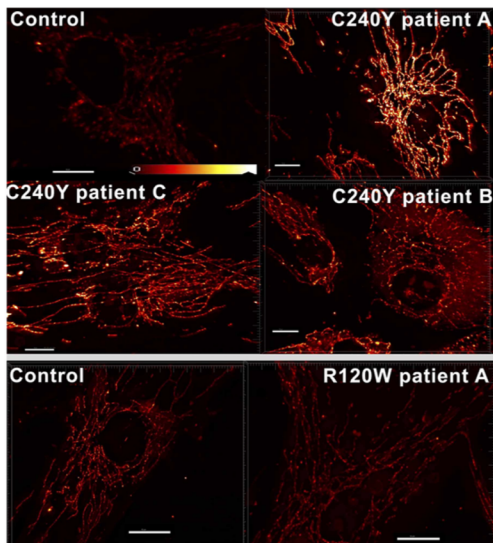
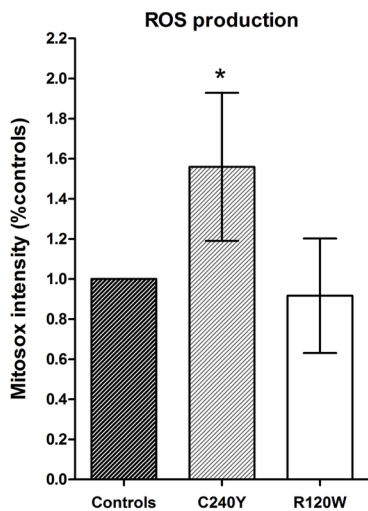
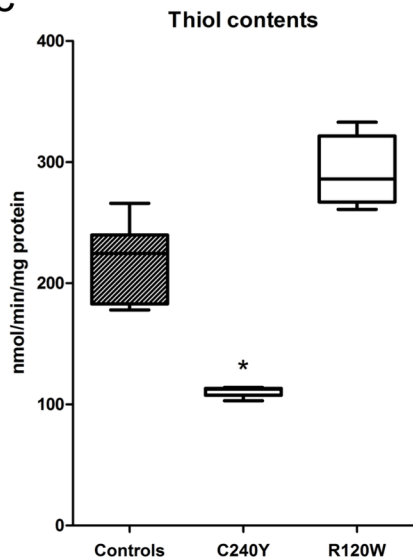
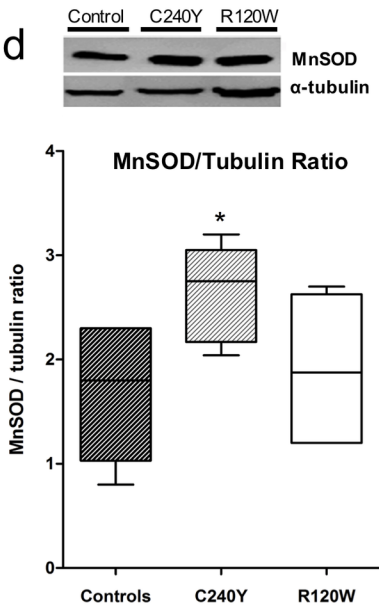
	Controls	C240Y	R120W
Citrate synthase (CS) activity (<i>nmol/min/mg protein</i>)	353 ± 67	404 ± 74	451 ± 44
Aconitase (<i>nmol/min/mg protein</i>)	10.48 ± 1.5	6.38 ± 0.9*	8.65 ± 1.8
Fumarase (<i>nmol/min/mg protein</i>)	8.0 ± 2.2	6.81 ± 0.5	5.63 ± 0.63
Aconitase/Fumarase	1.37 ± 0.33	0.93 ± 0.07*	1.53 ± 0.15
IDH/CS	0.20 ± 0.03	0.23 ± 0.04	0.26 ± 0.09

Enzymatic activities of the Krebs cycle were measured on CMT2K and control fibroblasts, and the aconitase/fumarase ratio considered as a marker of oxidative stress. Isocitrate dehydrogenase (IDH) activity was normalized with respect to citrate synthase (CS) activity.

a**b****c****d**

a**b****c**



a**b****c****d**

Resveratrol effect on complex I activity

